Adsorption (2012) 18:1–12
DOI 10.1007/s10450-011-9370-2

FTIR studies of butane, toluene and nitric oxide adsorption on Ag exchanged NaMordenite

Soledad G. Aspromonte · Eduardo E. Miró · Alicia V. Boix

Received: 18 February 2011 / Accepted: 12 September 2011 / Published online: 27 October 2011

Abstract In this work, we studied the adsorption of butane, toluene and nitric oxide on NaMordenite exchanged with different amounts of silver. The reactions that occurred when the adsorbed hydrocarbons interacted with NO and the effect of water adsorption were also addressed. Different silver species were formed after ion exchange and they were detected by TPR analysis. Highly dispersed Ag_2O particles were reduced at temperatures lower than 300 °C whereas Ag^+ exchanged ions showed two TPR peaks, which can be ascribed to species exchanged at different mordenite sites. The TPD experiments after adsorption of NO at 25 °C showed that the only desorbed species was NO_2 which was formed by the total reduction of Ag_2O particles. When the adsorbed butane was exposed to NO (1000 ppm), isocyanate species were formed on Ag^+ ionic sites as well as Ag^+–(NOx)–CO species. Toluene adsorption was stronger than butane since adsorbed toluene molecules were held even at 400 °C. The characteristic bands of the aromatic ring C=C bond was observed as well as that of methyl groups interacting with Ag^+ and Na^+ ions. However, the appearance of carboxylic groups at temperatures above 300 °C in inert flow indicated the partial oxidation of toluene due to Ag_2O species present in the samples. After contacting adsorbed toluene with NO, different FTIR bands correspond to organic nitro-compounds, isocyanate, cyanide and isocyanide species adsorbed on Ag^+ ions, were detected. The presence of water inhibited the formation of NO_2 species and the hydrocarbon adsorption on Na^+ sites but did not affect the toluene-Ag^+ interaction.

S.G. Aspromonte · E.E. Miró · A.V. Boix (✉)
Instituto de Investigaciones en Catálisis y Petroquímica – INCAPE (FIQ, UNL-CONICET), Santiago del Estero 2829, 3000, Santa Fe, Argentina
e-mail: aboix@fiq.unl.edu.ar

Keywords Hydrocarbon adsorption · Ag-Mordenite · FTIR spectroscopy · NOx selective reduction

1 Introduction

Hydrocarbons (HCs) and nitric oxides (NOx) are among the main pollutants generated in both mobile and stationary combustion emission sources. Three-way monolithic catalysts (TWC) are commonly used in automobiles because they achieve CO and HC oxidation together with NOx reduction for stoichiometric air/fuel (A/F) ratios. In stationary power sources, the Selective Catalytic Reduction of NO (SCR-NO) with ammonia is the most widely used commercial method to eliminate nitric oxide (Parvulescu et al. 1998). However, several problems still remain unsolved when these processes are employed. For example, TWCs are less efficient when the engine operates under lean conditions, which is the case of diesel engines. Another problem in the exhaust stream of automobiles is constituted by hydrocarbon emissions occurring when the temperature of the catalytic system is low, during the first 2 min after engine ignition, and before the TWC reaches its light-off temperature (Kanasawa 2004). In the case of stationary power sources, since ammonia is a corrosive gas, the use of hydrocarbons as a reducing agent could be highly desirable.

In the research literature seeking for a solution to the above mentioned drawbacks, zeolites have been the most widely used materials. For example, different metal-exchanged zeolites have been abundantly reported as promising catalysts for the SCR of NOx with hydrocarbon in the presence of O_2 excess. On the other hand, in the case of automobiles, a promising way to resolve the problem of HC emissions during the cold-start period is the installation of zeolitic traps, which are able to adsorb hydrocarbons during the cold period and release them once the light-off temperature of the converter is reached (Sarshar et al. 2009; Park et al. 2007; Wesson and Snurr 2009). Zeolites have also been extensively studied as adsorbents and catalysts due to their stability at high temperatures, their thermodynamic affinity to hydrocarbons and the high activity and selectivity to N_2 in the SCR of NOx (Son et al. 2000). However, the effect of water, which is inevitably present in combustion processes, represents an important drawback. Water is strongly adsorbed on high alumina zeolites, thus impeding the adsorption of reactive molecules in the active sites for the catalytic reactions. Moreover, metal-zeolites employed for the SCR of NOx are irreversibly damaged by the presence of water at high temperatures (Malka-Edery et al. 2001; Yeon et al. 2009; Iliyasm et al. 2007).

At present, the adsorption of gaseous contaminants is a very important research issue in view of the application of zeolites to solve environmental problems. Thus, the purpose of this work is twofold: (i) to contribute to the understanding of the physicochemical phenomena that take place when contaminants like nitric oxide and hydrocarbons are adsorbed on silver modified zeolites, and (ii) to gain insight into the effect of the presence of water. To this purpose, we selected toluene and butane as representatives of aromatic and aliphatic hydrocarbons that are usually present in the effluents of combustion processes. The study of the chemical interaction arising between adsorbed hydrocarbons with NO molecules of the gas phase are very important for the SCR-NOx process. Besides, water was added in the hydrocarbon stream in the experiment, because as said above, its presence is unavoidable. We selected Ag exchanged in Na-Mordenite as adsorbent because it has been reported that silver has a beneficial effect in hydrocarbon adsorption when water is present, and is an active component for the SCR-NOx reaction as well (Liu et al. 2001; Oliveira et al. 2009). Experiments with different silver loadings were performed and FTIR spectroscopy was used as a very powerful technique yielding important information about the mechanism of adsorption and reactions of the contaminants employed. In addition, temperature-programmed reduction (TPR) experiments were performed to assess the redox capacity of the solids which in turn helps to identify the different Ag species that are present.

2 Experimental

2.1 Preparation of Ag-mordenite catalysts

NaMOR with Si/Al = 6.5 was commercially obtained from Zeolyst International and used as the parent zeolite. A conventional Ag^+ ion exchange of NaMOR with $AgNO_3$ solution was carried out at room temperature (RT) in the dark for 24 hours using 150 ml of aqueous silver (I) nitrate solution (0.04–0.10 M) to exchange 4 g zeolites each time. The samples were filtered, washed with deionized water, dried overnight at 120 °C and then calcined in O_2 flow at a heating rate of 0.5 °C/min from RT to 500 °C; then, the temperature was kept constant for 2 hours. Hereafter, the catalyst will be designated as Ag(x)M where 'x' represents the silver content (wt%). Samples with 5, 10 and 15 wt% Ag were obtained, the exchange degree being 17.8, 35.5 and 53.1%, respectively. The silver content was determined by Atomic Absorption Spectrometry Flame (AASF). Besides, a mechanical mixture between Ag_2O and NaMOR was prepared to obtain a solid with 15 wt% Ag. This mixture was used as the reference sample in the TPR experiments.

2.2 Temperature-programmed reduction (TPR)

TPR measurements were performed in a flow system (Okhura TP-2002 S instrument) equipped with a TCD detector for monitoring the H_2 consumption from a feed stream containing 5% H_2 in Ar. Normally, 0.1 g of fresh samples was placed in a quartz tube of 8 mm (i.d.) and calcined in situ with O_2 from RT up to 500 °C with a heating rate of 0.5 °C/min. It was kept at 500 °C for 2 hours, and was then cooled down to RT. The TPR experiments started at 30 °C up to 900 °C with a heating rate of 10 °C/min.

2.3 Temperature-programmed desorption of NO (NO-TPD)

These experiments were carried out using 100 mg of calcined sample in a flow system. Prior to the NO-TPD experiment, the catalyst was pretreated in inert flow at 500 °C for 2 hours and then cooled down to room temperature (RT). NO chemisorption was performed by passing 1000 ppm of NO in He at 25 °C for 1 hour. The TPD measurements were carried out up to 600 °C with a heating rate of 5 °C/min in inert flow. The concentration of NOx species was measured by FTIR at the reactor outlet. Spectra were recorded using a FTIR Thermo Matso Genesis II, equipped with a gas IR cell having a 15 cm path length (47 ml volume) and CaF_2 windows. A total of 100 scans were collected with a nominal resolution of 1 cm^{-1}.

2.4 FTIR studies

Through FTIR measurements, the interactions between hydrocarbons and Ag species were studied by means of different adsorption-desorption experiments. FTIR spectra were collected using a Shimadzu 8108 M spectrometer, IR Prestige-21 model, equipped with a high sensitive DLATGS detector. A 30 mg sample was pressed into a self-supported disc of approximately 1 cm of diameter and placed in a sample holder at the center of the cell. The quartz cell had an inlet and outlet allowing gas flow. This was externally heated and the temperature was measured with a thermocouple placed in close proximity of the catalyst sample. Absorbance spectra were collected in the single-beam mode by recording 80 scans at a resolution of 2 cm^{-1}.

Before each experiment, catalyst samples previously calcined at 500 °C were pretreated in situ with inert flow at 400 °C for 12 hours; they were then cooled down to adsorption temperature. The spectra of the clean sample surface were collected and then the HC adsorption was carried out. In the case of the linear HC, the adsorption was performed with 1500 ppm of C_4H_{10}/He at RT. Instead, aromatic HC adsorption studies were conducted by exposing catalyst samples to a stream of 8000 ppm of toluene at 100 °C. This concentration was obtained by flowing inert flow through two successive saturators which contained pure toluene. In some experiments, 0.5% of water was also introduced in the feed stream. In all cases, after adsorption the sample was flushed with inert flow at the adsorption temperature to remove the physisorbed species and then, the spectra of the adsorbed HCs were obtained.

Once the HC was adsorbed, there were two separate measurements. The first one was carried out by sweeping the HC adsorbed with inert flow for 30 minutes at different temperatures to study the thermal stability of adsorbed butane or toluene. On the other hand, the second experiment was performed flowing 1000 ppm NO in He for 30 minutes at different temperatures to analyze NOx–HC interactions.

3 Results

3.1 Reducibility of Ag species

The properties of the active sites are related to the different species of Ag present in the catalysts. Temperature-programmed reduction allows identifying these species. Table 1 and Fig. 1 show the results obtained by TPR for Ag(x)M catalysts and for the standard sample. The reduction profiles exhibit peaks in the three temperature regions which can be attributed to different silver species.

The main reduction peaks close to 222 °C (region I) could correspond to small highly dispersed particles which may be associated with Ag_2O species (Berndt et al. 1998). Another small peak present in this region suggests a different interaction between the oxide particles with the channels of the support (Bethke and Kung 1997; Baek et al. 2004). From the XRD pattern (not shown), the average size of Ag_2O particles was estimated on the Ag_2O/M reference sample, which was approximately 38 nm. However, no Ag species were detected in the Ag(x)M samples. The reduction at temperatures between 300 °C and 600 °C (region II) is generally attributed to Ag^+ ions at exchange positions. Besides, there is a small fraction above 600 °C (region III) that could be assigned to Ag^+ ions located at very stable sites with high coordination, in which the cation strongly interacts with the zeolitic structure. These two peaks could be ascribed to species exchanged at different mordenite sites, probably in the main channels and in the side pockets, respectively (Mortier 1977).

The H_2 consumption/Ag molar ratio calculated for Ag(15)M is close to 0.5 which indicates the complete re-

Table 1 Reducibility of silver species in Ag(x)M samples

Catalyst[a]	H_2/Ag (T_{max}, °C)[b] 25–300 °C	300–600 °C	>600 °C	H_2/Ag_{total}
Ag_2O/M	0.50 (190)	–	–	0.50
Ag(5)M	0.14 (221)	0.17 (406)	0.05 (780)	0.36
Ag(10)M	0.18 (222)	0.24 (404)	0.03 (770)	0.45
Ag(15)M	0.22 (222)	0.19 (443)	0.09 (757)	0.50

[a] The Ag(x)M samples were calcined at 500 °C in O_2 flow. The Ag_2O/M sample was dehydrated at 500 °C in N_2 flow

[b] Maximum temperature of reduction in each region (°C)

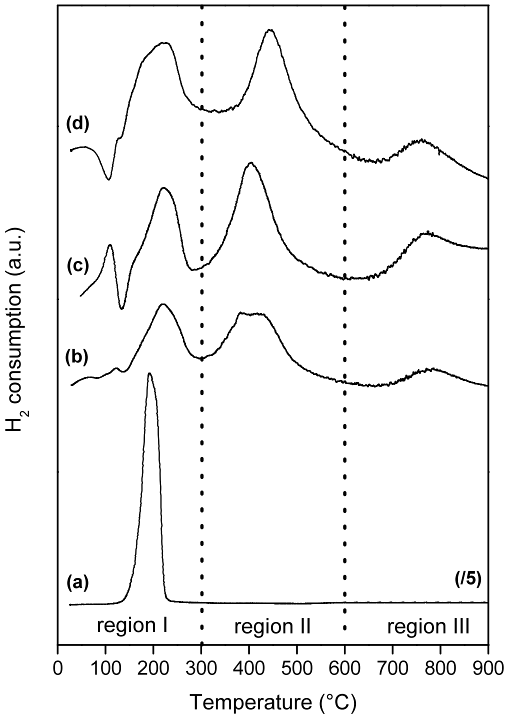

Fig. 1 TPR profiles (a) Ag_2O/M (mechanical mixture) and calcined samples: (b) Ag(5)M, (c) Ag(10)M and (d) Ag(15)M

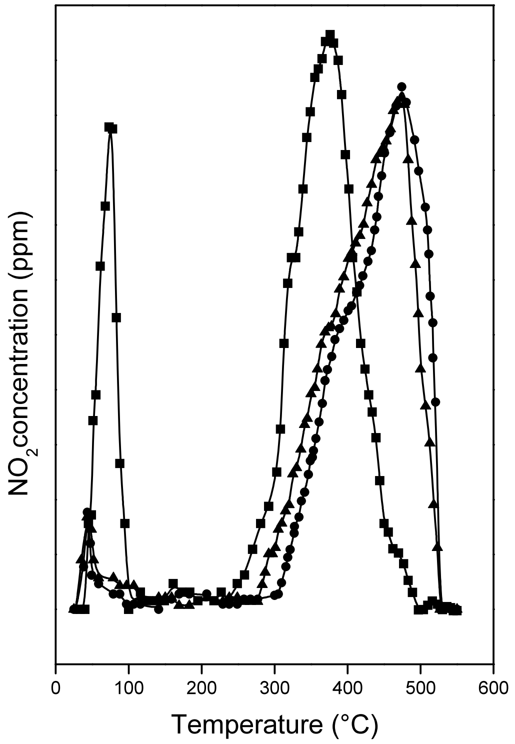

Fig. 2 Temperature-Programmed Desorption (TPD) of NO adsorbed at 25 °C on (■) Ag_2O/M, (●) Ag(5)M and (▲) Ag(15)M

duction of Ag^+ species to their metallic state (Table 1) and coincides with those obtained for the reference sample, Ag_2O/M. However, in the samples with 5% and 10% wt. of silver the H_2/Ag ratio is less than 0.5.

3.2 Temperature-programmed desorption of NO (NO–TPD)

Figure 2 displays the desorption profiles obtained after NO adsorption at 25 °C on Ag(5)M and Ag(15)M and compared with the reference sample. The y-axis refers to the concentration at the reactor outlet of NO_2 normalized to the Ag_2O content. The representative curve of NO-TPD has a low intensity peak below 100 °C and another above 300 °C. Samples Ag(x)M show a shift of the second peak toward higher temperatures with respect to the reference Ag_2O/M, which could be attributed to the interaction of NO with different Ag species dispersed in the structure.

Desorbed species were analyzed at the exit of the reactor and the only signal detected at 1628 cm^{-1}, belongs to NO_2 species. This suggests that adsorbed NO is oxidized in the presence of Ag_2O oxides.

It was possible to calculate the NO_2/Ag_2O molar ratio (Table 2) taking into account both the area under the TPD curve which is related to the µmoles of NO_2 desorbed and the reduction peaks below 300 °C that correspond to Ag_2O particles. The values close to 1 suggest the complete oxidation of NO molecules adsorbed on Ag_2O.

Table 2 NO-TPD and TPR results

Catalyst	µmol NO_2[a]	µmol Ag_2O[b]	NO_2/Ag_2O
Ag_2O/M	78	70	1.11
Ag(5)M	6.3	6.5	0.97
Ag(15)M	31	30.6	1.01

[a] µmoles calculated by NO-TPD

[b] µmoles calculated by TPR

3.3 FTIR characterization of hydrocarbons adsorbed on Ag-exchanged mordenite

3.3.1 Butane adsorption followed by inert sweep

Figure 3 displays spectra obtained after butane adsorption at 100 °C on NaMOR and Ag-exchanged samples followed by inert sweep at 100 °C. The IR band observed at 2934 cm^{-1} is assigned to the asymmetric C–H stretching of the $–CH_2$ group in the butane molecule [ν^a (CH_2)], while the bands at 2960 and 2868 cm^{-1} correspond to the asymmetric and symmetric –C–H stretching of the methyl group [ν^a (CH_3) and ν^s (CH_3)], respectively. On the other hand, the bands at 1466 and 1381 cm^{-1} are assigned to the deformation of the C–H bonding of the CH_x group (δ CH_2/CH_3) (Müslehiddinoglu and Vannice 2004).

Moreover, by increasing the silver content the more intense absorption bands in the IR spectra can be observed (3000–2750 cm^{-1} region), which indicates the preferential interaction between hydrocarbon and silver ions.

In the low wavenumber region (1550–1300 cm^{-1}), the Ag(5)M sample (Fig. 3, spectrum b) shows a main peak at 1466 cm^{-1} that corresponds to the butane interaction with Na^+ sites (remaining in the Ag(5)M) and an additional band at 1460 cm^{-1} due to the interaction with Ag^+ ions present in the samples, which increases its intensity with the Ag loading.

After flowing He at 150 °C, no FTIR bands of adsorbed butane could be observed, which suggests a weak butane adsorption on the Ag(x)M samples.

3.3.2 Toluene adsorption followed by inert sweep

Figure 4 shows the FTIR spectra of toluene adsorbed at 100 °C and desorbed in inert flow at 200, 300 and 400 °C for the NaMOR support.

In the high wavenumber region (Fig. 4A), weak bands are observed above 3000 cm^{-1} (3033 and 3073 cm^{-1}) which correspond to the C–H stretching of the toluene aromatic ring. Below 3000 cm^{-1}, the signals at 2924 and 2877 cm^{-1} can be assigned to the –C–H stretching of the methyl group. In the low wavenumber region (Fig. 4B), there is a signal

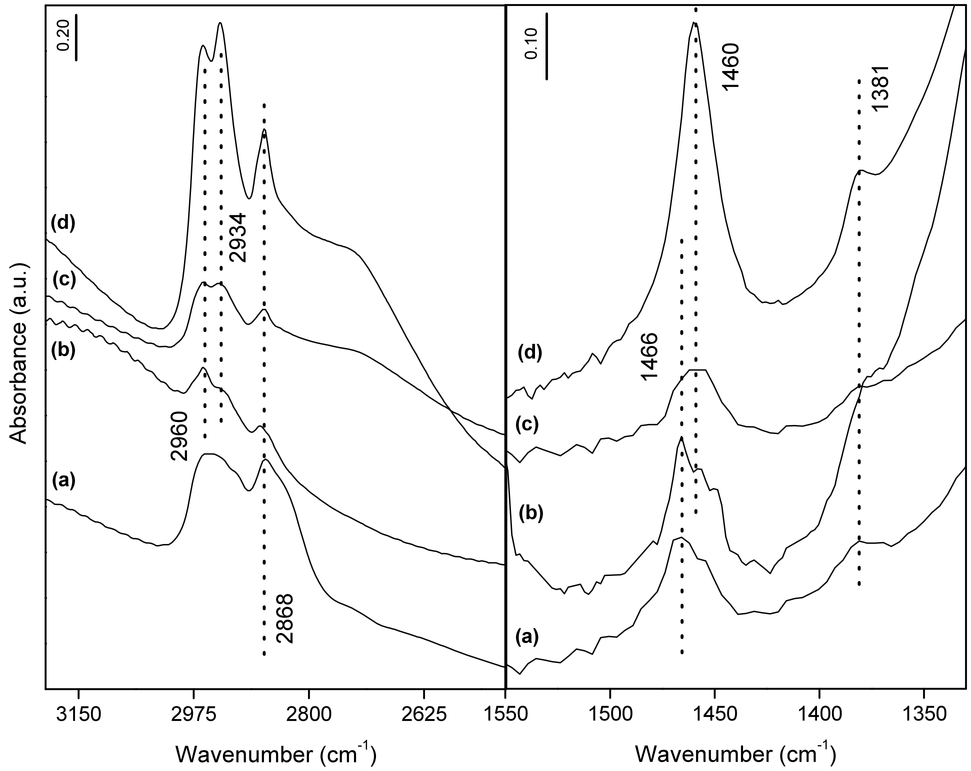

Fig. 3 FTIR of butane adsorbed and purged with inert flow at 100 °C on (*a*) NaMOR, (*b*) Ag(5)M, (*c*) Ag(10)M and (*d*) Ag(15)M

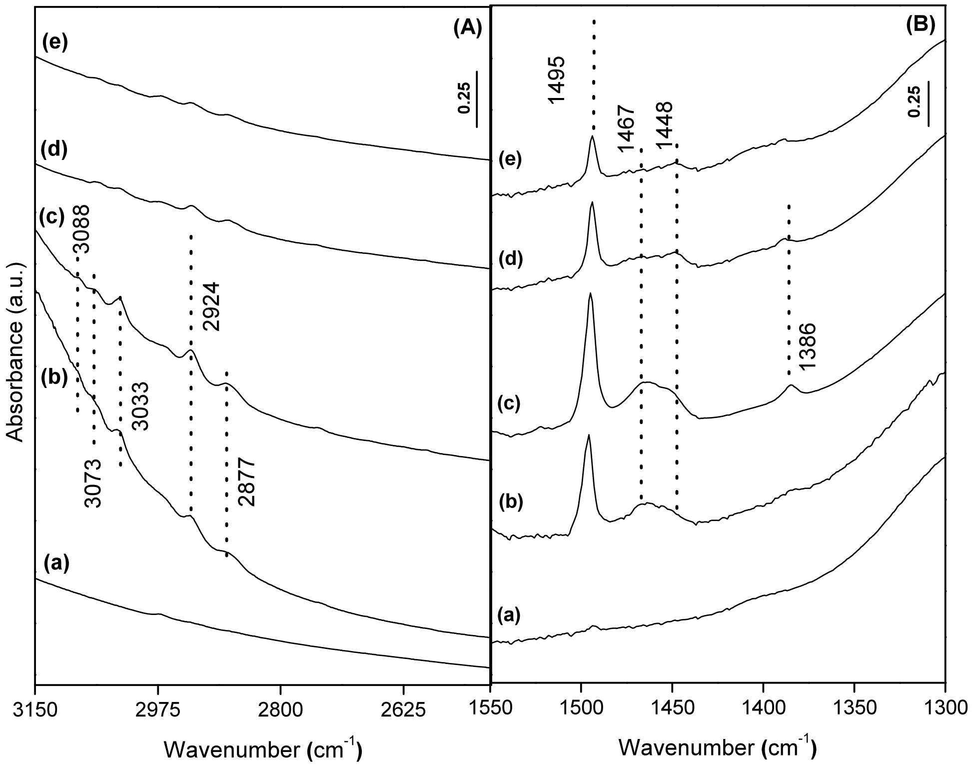

Fig. 4 FTIR of toluene adsorbed on NaMOR; (*a*) support pre-treated in inert flow at 400 °C, (*b*) toluene adsorption and purge with inert flow at 100 °C, toluene desorption in inert flow at (*c*) 200 °C, (*d*) 300 °C and (*e*) 400 °C

at 1495 cm^{-1} attributed to the vibrational modes of the aromatic ring C=C stretching interacting with Na^{+} ions of the NaMOR support. A shift of 10 cm^{-1} to low wavenumbers in comparison with gas phase toluene (1506 cm^{-1}) can be observed. There is also a broad band centered at 1467 cm^{-1} with a signal at 1386 cm^{-1} which corresponds to the asym-

Fig. 5 FTIR of toluene adsorbed on NaMOR (spectrum *a*) and Ag(15)M (spectra *b*–*d*), purge with inert flow at 100 °C (*a*, *b*), 200 °C (*c*), 300 °C (*d*) and 400 °C (*e*)

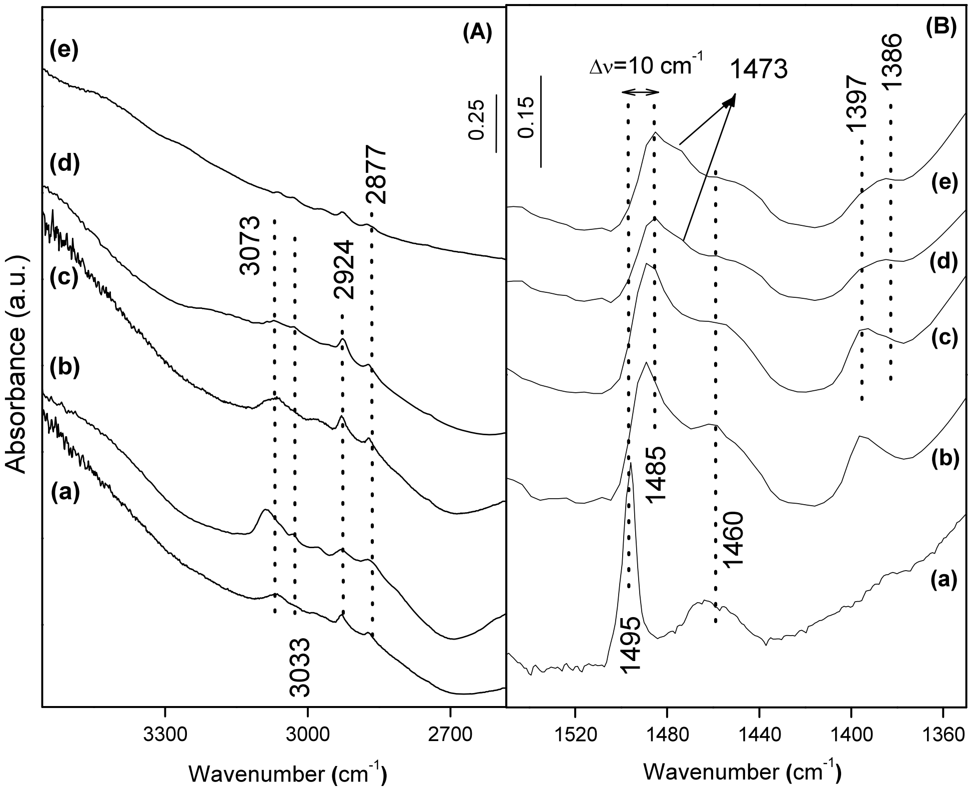

metric deformation of the C–H bonding of the methyl group in the toluene molecule (Poucher 1981), and a shoulder at 1448 cm^{-1} assigned to the stretching of the aromatic ring. Figure 5 shows the FTIR spectra of toluene adsorbed at 100 °C and desorbed in inert flow at 200, 300 and 400 °C for the Ag(15)M catalyst. Toluene adsorbed on Ag(15)M (Fig. 5—spectrum b) exhibits a shoulder at 1485 cm^{-1} which can be attributed to toluene interacting with Ag^+ ions that shift at lower wavenumbers compared to the band observed in NaMOR at 1495 cm^{-1} (spectrum a). The presence of this latter band, even though the temperature rises to 400 °C, indicates a strong interaction between Ag^+ ions and the toluene molecule. Besides, the signals centered at 1460 and 1397 cm^{-1} assigned to the deformation of the C–H bonding of the $-\mathrm{CH}_3$ group shift towards lower wavenumbers with the increase of temperature (spectra c–e).

When the temperature rises to 300 °C (Fig. 5, spectra d and e), a shoulder at 1473 cm^{-1} appears, which can be assigned to the vibrations of the symmetric C=O stretching of carboxylate groups. However, this signal is not observed in the NaMOR sample (Fig. 4). In the samples with lower silver loading, Ag(5)M and Ag(10)M, the spectra of toluene adsorbed at different temperatures show similar bands. Figure 6 summarizes the spectra of adsorbed toluene at 400 °C in inert flow on Ag(x)M samples and compares them with that in NaMOR. In the silver exchanged mordenite, there appear the characteristic bands at 1485, 1448 and 1386 cm^{-1} associated with the interaction between toluene

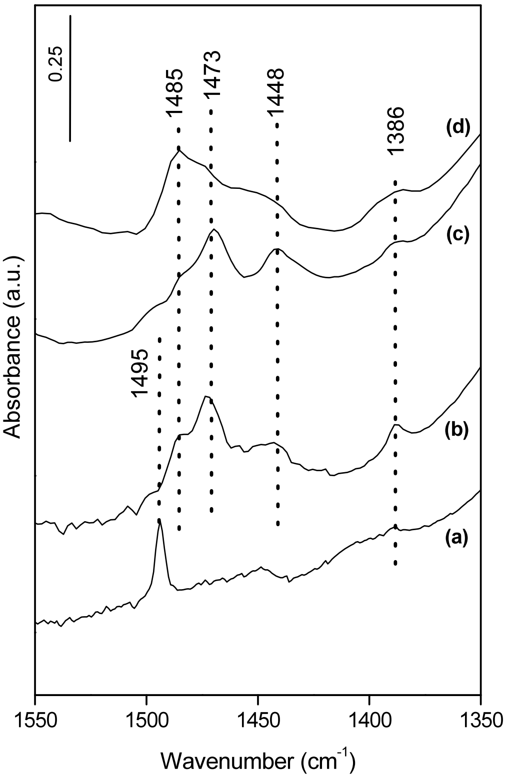

Fig. 6 FTIR of toluene adsorbed at 100 °C and desorbed at 400 °C in inert flow on (*a*) NaMOR, (*b*) Ag(5)M, (*c*) Ag(10)M and (*d*) Ag(15)M

molecules with Ag^+ ions. The appearance of a stronger band at 1473 cm^{-1} suggests the partial oxidation of toluene at 400 °C in the presence of silver species, like Ag_2O sites (Wichterlová et al. 2005; Hadjiivanov 2000).

3.3.3 Butane adsorption followed by sweep with 1000 ppm NO/He flow

Figure 7 shows the spectra of adsorbed butane on Ag(x)M samples and NaMOR treated at 100 °C in butane/He flow, followed by a sweep with 1000 ppm of NO/He and then in inert flow. In all the Ag(x)M samples, the bands corresponding to adsorbed butane (2700–3000 cm^{-1} region) with a broad signal between 2250 and 2100 cm^{-1} are observed. The shoulder at 2240 cm^{-1} could be attributed to isocyanate (–NCO) species adsorbed on ionic sites Ag^+, whereas the band at 2181 cm^{-1} suggests the presence of adsorbed Ag^+(NOx)–CO species (Hadjiivanov 1998), which proves the reaction at low temperature between adsorbed butane, the oxygen of Ag_2O species and NO molecules of the gas phase. There were no characteristic bands of NOx, NO_2, NO_3^- and NO_2^- adsorbed species, which normally appeared in the 2000–1300 cm^{-1} region.

3.4 Toluene adsorption followed by sweep with 1000 ppm NO/He flow

Figure 8 shows the signals obtained for the Ag(5)M and Ag(15)M samples at 400 °C in inert flow and the spectra

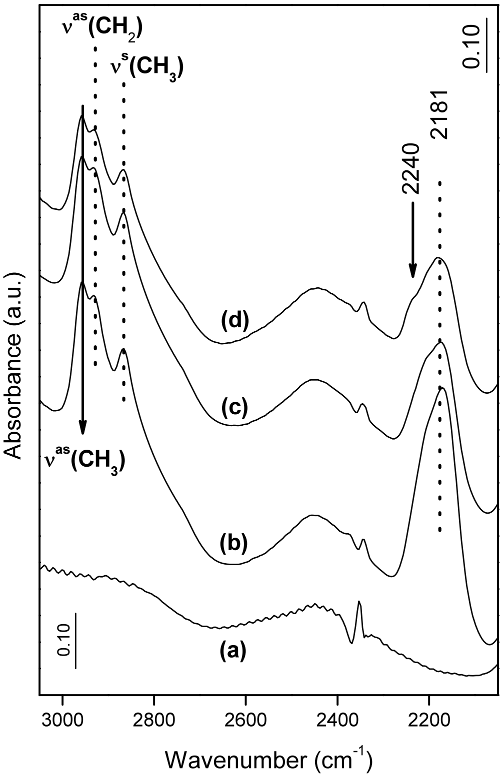

Fig. 7 FTIR measured after butane adsorption followed by NO/He flow at 100 °C on (*a*) NaMOR, (*b*) Ag(5)M, (*c*) Ag(10)M and (*d*) Ag(15)M

Fig. 8 FTIR of toluene adsorbed on (**A**) Ag(5)M and (**B**) Ag(15)M; (*a*) purge in inert flow at 400 °C; desorption of toluene in NO/He flow at 250 °C (*b*) and 400 °C (*c*)

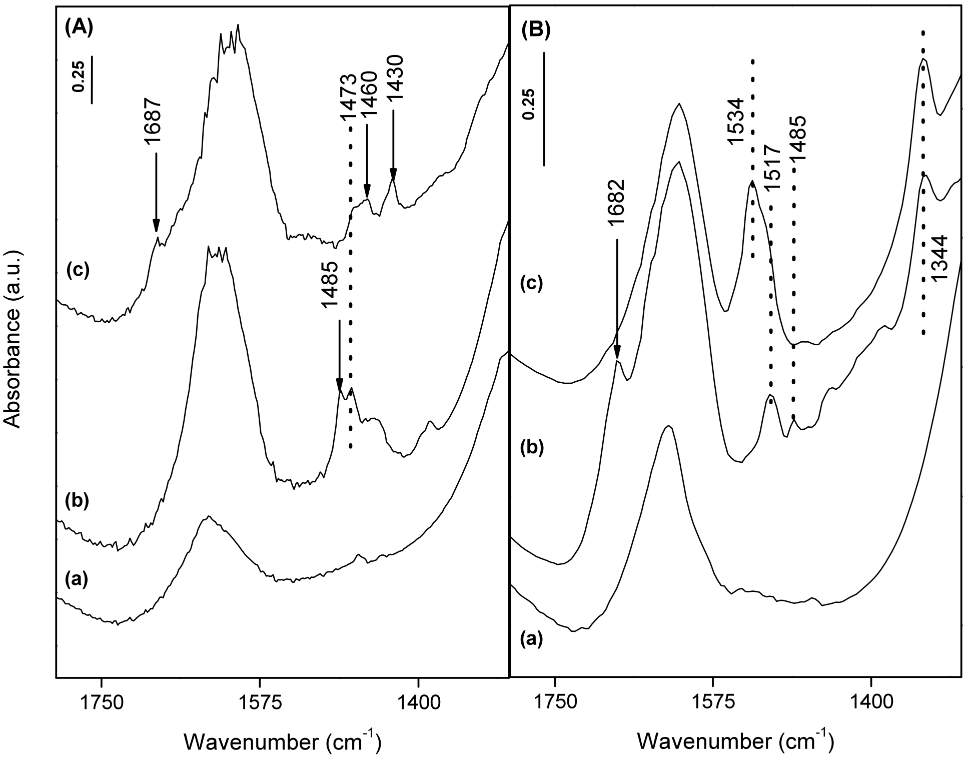

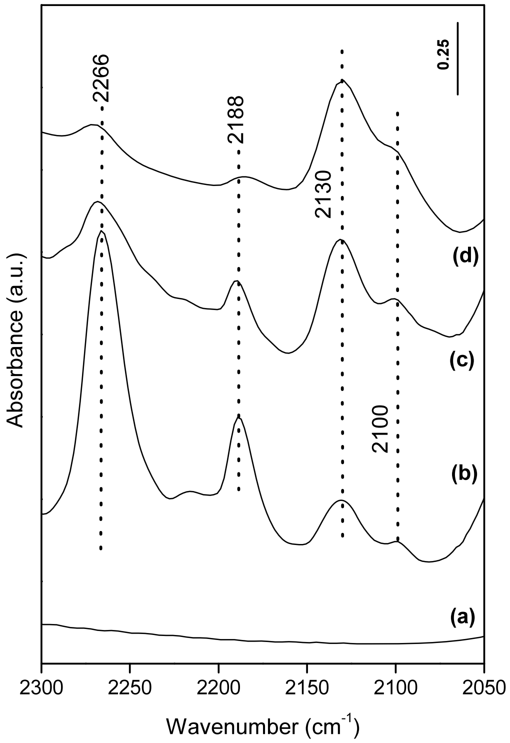

Fig. 9 FTIR of toluene adsorbed at 100 °C and desorbed at 400 °C in NO/He flow (1000 ppm) on (*a*) NaMOR, (*b*) Ag(5)M, (*c*) Ag(10)M and (*d*) Ag(15)M

of adsorbed toluene and swept at 250 °C (spectrum b) and 400 °C (spectrum c) in NO/He flow. A peak at 1485 cm^{-1}, corresponding to the aromatic ring C=C stretching interacting with Ag^+ ions, is present at 250 °C in both samples.

In the Ag(5)M catalyst (Fig. 8A), there appear two signals at 1460 and 1430 cm^{-1} which are assigned to surface NO_2^- species (nitro, nitrite or nitro-nitrite form). In addition, at 400 °C there appears a band at 1687 cm^{-1} associated with NO_2 species (Fig. 8A, spectrum c). The vibration of the C=O asymmetric stretching of the carboxylate group (1473 cm^{-1}) is observed above 250 °C (Hadjiivanov 1998; Yeom et al. 2007).

By increasing the silver content to 15 wt% (Fig. 8B), it is possible to see the adsorbed NO_2 species at 250 °C (spectrum b). A broad signal appears in the 1550–1500 cm^{-1} region, accompanied by another band at 1344 cm^{-1}. These signals are more intense at 400 °C (spectrum c) and correspond to the vibrations of organic nitro-compounds (R–NO_2) (Yeom et al. 2007). Besides, a widening of the band in the 1750–1530 cm^{-1} region is observed. It might be an overlap between the signals at 1642 cm^{-1} of adsorbed water and the signal at 1626 cm^{-1} which belongs to the NaMOR structure.

In addition, Fig. 9 shows new bands in the 2300–2050 cm^{-1} region, which correspond to intermediate species produced by the reaction between the adsorbed toluene and NO at 400 °C. The band at 2266 cm^{-1} is usually assigned to the stretching vibration of isocyanate groups (N=C=O) on Ag^+ ions while the signals at 2130 and 2100 cm^{-1} are assigned to cyanide (Ag–CN) and isocyanide (Ag–NC) species adsorbed on the catalyst surface, respectively (Dorado et al. 2005; Yeom et al. 2007; Shimizu et al. 2001; Tamm et al. 2008; Thibault-Starzyk et al. 2009).

The bands shown in the 2200–2150 cm^{-1} region belong to the vibration modes of monocarbonyl –(CO) and –$(CO)_2$ species formed on highly coordinated unsatured Ag^+ ions or small Ag° particles (Zhanpeisov et al. 2003; Hadjiivanov and Vayssilov 2002). The appearance of water as reaction product between hydrocarbons and NO molecules decreases the intensity of bands and shifts them to shorter wavenumbers promoting the formation of Ag^+–(H_2O)–(CO) or of Ag^+–(NO_x)–(CO) species (Hadjiivanov and Vayssilov 2002).

3.4.1 *Effect of water on adsorption properties*

The effect of the presence of water on the adsorbed species on Ag(x)M catalysts is of great importance for environmental applications. This is because water is present in significant amounts in a typical exhaust emission from combustion process and the competitive adsorption with hydrocarbons may block the active sites of the catalysts. Thus, a gas mixture of 8000 ppm of toluene with 0.5% of H_2O was introduced into the cell.

Figure 10 shows the FTIR spectra of toluene and water co-adsorbed at 100 °C on Ag(15)M and desorbed in inert flow at 200, 300 and 400 °C. An increase in the width of the band located between 1700 and 1550 cm^{-1} is observed when the water is added in the reactant stream. This broadening is the overlap of three bands, one at 1642 cm^{-1} of water bending vibration, another at 1626 cm^{-1} due to the zeolite structure, and a third one at 1595 cm^{-1} which belongs to the aromatic ring C=C stretching interacting with Ag^+ ions. In addition, bands at 1465 and 1388 cm^{-1} can be observed, which correspond to the interaction of the methyl group with cations Na^+ and Ag^+. Figure 10, spectrum b, shows signals at 1595 and 1488 cm^{-1} due only to the toluene adsorption on Ag^+ ions. Therefore, it can be inferred that the presence of H_2O inhibits the interaction between the aromatic ring with Na^+ sites, but does not affect this interaction with Ag^+ ions. The broad band around 1642 cm^{-1} decreases when the temperature increases from 200 °C (spectrum c) to 400 °C (spectrum e) and only the signal at 1626 cm^{-1} remains, corresponding to the structure of NaMOR. In addition, the peaks assigned to the C=O group as a result of toluene oxidation on Ag sites (1575 and 1473 cm^{-1}) are observed above 300 °C.

Figure 11 presents the spectra obtained after coadsorbing toluene and water in the Ag(15)M sample, which was later

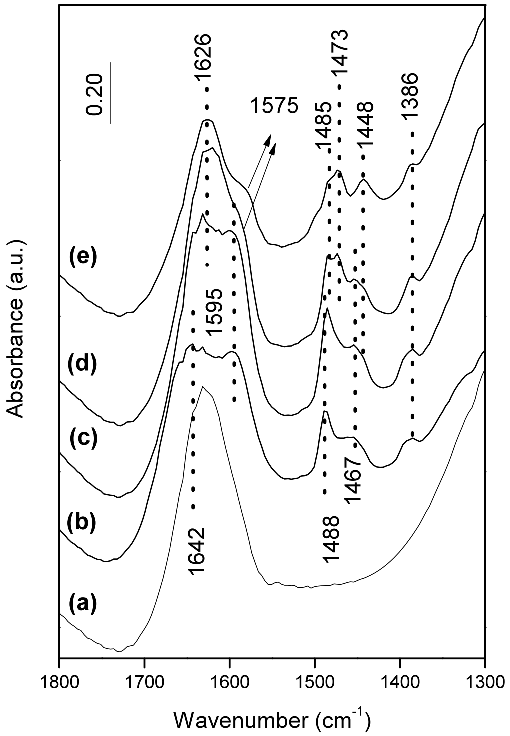

Fig. 10 FTIR of toluene and H_2O co-adsorbed on Ag(15)M; (*a*) support pre-treated in inert flow at 400 °C, (*b*) adsorption of toluene and H_2O at 100 °C and purge with inert flow at 100 °C, (*c*) desorption in inert flow at 200 °C, (*d*) 300 °C and (*e*) 400 °C

swept in NO flow at different temperatures. The spectral region between 1750 and 1300 cm^{-1} (Fig. 11A) shows the characteristic bands of toluene (1485, 1448 and 1386 cm^{-1}) and water bending vibration at 1642 cm^{-1}. Bands at 1575 and 1472 cm^{-1}, corresponding to the partial oxidation of toluene on Ag sites are also observed. However, the presence of water inhibits the formation of NO_2 species. At the same time, Fig. 11B shows the 2400–2000 cm^{-1} region for isocyanate (2266 cm^{-1}) and cyanide (2130 cm^{-1}) groups adsorbed on Ag^+ ions, which denote intermediate compounds of the NO selective reduction. Figure 11B shows the peak at 2191 cm^{-1} which can be assigned to the vibration modes of monocarbonyl –(CO) and $-(CO)_2$ species formed on highly coordinated unsatured Ag^+ ions or small Ag° particles (Zhanpeisov et al. 2003; Hadjiivanov and Vayssilov 2002).

4 Discussion

Ag(x)M samples prepared by ion exchange have different Ag species. Through TPR, Ag_2O particles highly dispersed in the zeolite structure and Ag^+ ions at exchange sites can be found. When the silver content increases, the reducibility of the Ag_2O species does not change since the maximum temperature is always 222 °C. However, the formation of silver oxide is favored by a higher concentration of ions in solution during the ion exchange, because the proportion of this

Fig. 11 FTIR of toluene and H_2O co-adsorbed on Ag(15)M; (*a*) support pre-treated in inert at 400 °C, (*b*) adsorption of toluene and H_2O and purge with inert at 100 °C, (*c*) desorption in NO flow (1000 ppm) at 250 °C and (*d*) 400 °C

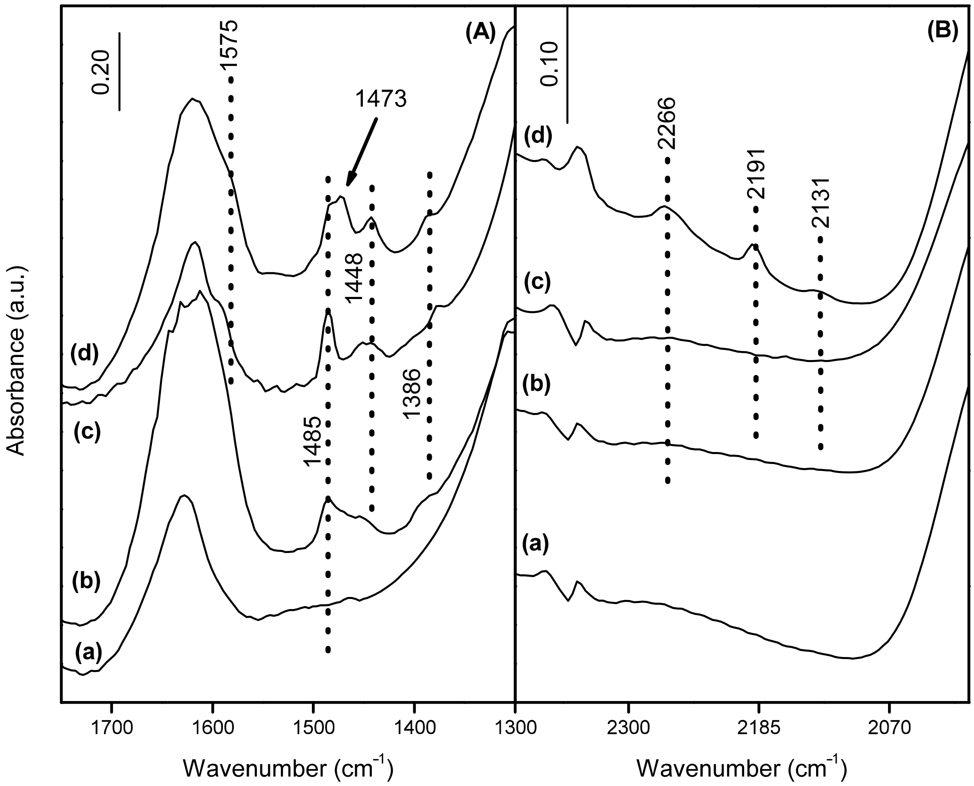

oxide increases from 0.14 to 0.22 for 5 to 15 wt% Ag, respectively (Table 1).

Probably, the Ag_2O species are formed from the thermal decomposition of Ag(OH) species during the calcination process, according to the following reactions (Schoonheydt et al. 1976):

$$Ag^+ + OH^- \rightarrow Ag(OH) \quad \text{(in aqueous solution)} \tag{1}$$

$$2Ag(OH) \rightarrow Ag_2O + H_2O \quad \text{(in the pores during calcination)} \tag{2}$$

This pathway produces very small particles of silver oxide which are highly dispersed inside zeolite channels and are not detected by XRD.

On the other hand, Ag^+ ions are preferentially exchanged in the main channel of the Na-mordenite structure, which is reduced at moderate temperatures. A smaller fraction is at more stable sites (side-pocket) where Ag^+ ions strongly interact with the atoms of the structure. So, in the Ag(15)M sample almost half the silver species are part of the Ag_2O particles and the rest are at the exchange site. When the exchange level is lower, the proportion of Ag^+ ions reduced in the 300–600 °C range hardly changes, the amount of silver oxide decreases, and some silver ions remain unreduced at 900 °C.

Ag_2O completely oxidizes NO to NO_2 using a redox process which was tested by adsorption of NO and TPD. The NO_2 species formed are more strongly adsorbed on small Ag° particles dispersed inside the zeolite framework, since the maximum desorption temperature is higher than the sample prepared by mechanical mixing.

The oxidation of NO adsorbed on Ag_2O could be carried out according to the following reactions:

$$NO(g) \rightarrow NO(ads) \tag{3}$$

$$NO(ads) + Ag_2O(s) \rightarrow NO_2(ads) + 2Ag^\circ(s) \tag{4}$$

$$NO_2(ads) \rightarrow NO_2(g) \tag{5}$$

The value close to 1 proves the proposed stoichiometry (Reaction (4)).

Henriques et al. (2001) reported that the NO^+ ions are generated from NO + O_2 co-adsorbed on Na-Mordenite by the replacement of Na^+ ions in cationic positions in the main channels, together with the formation of sodium nitrate. But Na^+ ions in the side pockets were not affected, and no formation of nitrate ions was observed in them. They reported as well the formation of NO_2 by the reaction of NO with O_2 in the gas phase.

In our study, the presence of NO_2 in the gas phase is only related to the reaction between the NO added in the input flow and the oxygen from Ag_2O species. In Ag exchanged mordenite samples, there is a small fraction of Na^+ ions remaining, probably located in the side-pockets. These sites are less active than those located in the main channel. Moreover, the formation of sodium nitrate reported by Henriques et al. (2001) is not observed in our case.

The FTIR study shows that the strength of the interaction between the adsorbed hydrocarbon in the Ag(x)M samples depends on the HC nature (linear or aromatic) as well as on the Ag loading present in the solids.

Butane is weakly adsorbed at 100 °C in the Ag(x)M samples because the typical vibrations of C–H bonds disappear at 150 °C in inert flow. However, it could be observed that the higher the silver loadings in the samples, the higher the band intensity of adsorbed butane (Fig. 3). However, the interaction strength between methyl group and structure is weak.

On the other hand, the adsorbed toluene shows the characteristic vibrations of the C–H bonds of the methyl group and the C=C double bond of the aromatic ring. Toluene has a stronger interaction with the Na^+ and Ag^+ ions compared with butane. The most intense band is associated with the C=C stretching of the aromatic ring; it is centered at 1495 cm^{-1} (in NaMOR) and shifts to 1485 cm^{-1} when increasing the silver loading (Figs. 4 and 5). Toluene remains adsorbed up to 400 °C. Besides, as from 300 °C there appears a new band associated with the C=O bonds which correspond to carboxylic groups (1473 cm^{-1}), generated by hydrocarbon oxidation on Ag_2O species (Fig. 6).

At low temperature, the adsorbed toluene on Ag(x)M shows the interaction between the methyl group with Ag^+ sites (1397 cm^{-1}) and as the temperature increases, the interaction with Na^+ ions (1386 cm^{-1}) prevails. However, the band assigned to the interaction between the C=C bond and the Ag^+ ions predominates at high temperatures compared to the corresponding interaction with Na^+ sites (Fig. 5). This is possibly due to the fact that the Ag^+ ions ([Kr] $4d^{10}5s^0$) are able to activate the adsorbed toluene containing π electrons through the donation of d electrons to $\pi*$ antibonding orbitals of the toluene molecule (Kulkulska-Zajac and Datka 2008; Lucolano et al. 2008). In the same vein, the toluene molecules that interact more weakly with Na^+ ions are capable of being oxidized on Ag_2O forming carboxylic species (Fig. 6). Based on the results obtained, the reaction scheme presented in Fig. 12 might be suggested. When adsorbed hydrocarbons are swept with a NO/He mixture, intermediate species of the SCR of NOx are observed. With butane, the signals detected correspond to adsorbed isocyanate and Ag^+(NOx)–CO. On the other hand, when the hydrocarbon is more reactive such as toluene, the signals detected correspond to organic nitro-compounds, cyanides and isocyanides adsorbed on Ag^+ ions.

However, by sweeping with NO/He after adsorbing toluene or butane, no nitrate species are formed because the Ag^+ and Na^+ sites are occupied with HC at the time of sweeping with NO/He.

Fig. 12 Scheme of possible reactions

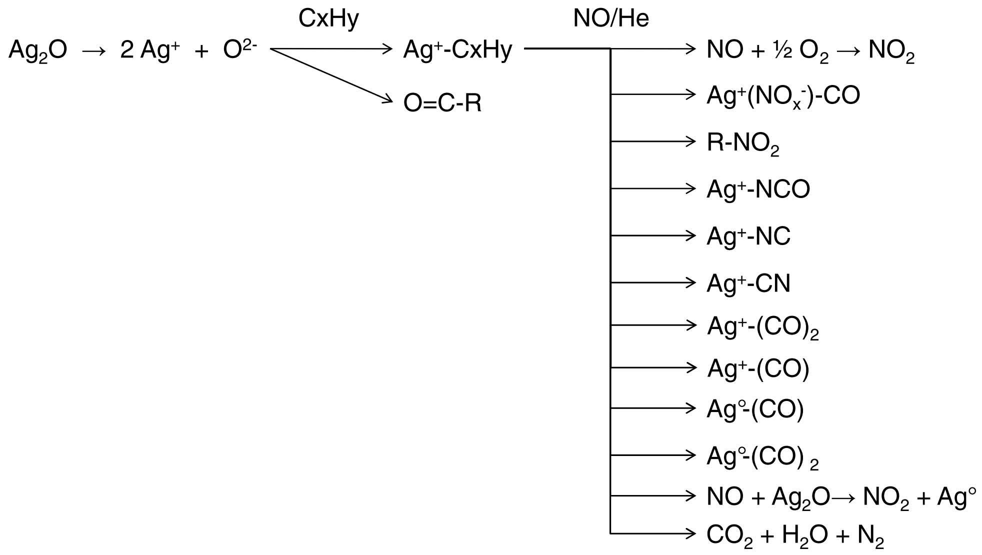

On the other hand, the formation of water over 250 °C is due to the interaction between toluene and NO according to the following reaction:

$$C_7H_8 + 18NO \rightarrow 7CO_2 + 4H_2O + 9N_2 \qquad (6)$$

It is clear that the aggregate of H_2O has no effect on toluene–Ag^+ interactions. On the contrary, hydration affects Na^+ sites because the band at 1495 cm^{-1} disappears after adsorbing toluene and water at 100 °C. Hydration weakens the interaction between Na^+ and toluene (Fig. 10). Although toluene is co-adsorbed with water, it is able to react with NO molecules of the gas phase above 300 °C.

5 Conclusions

Different silver species are present in Ag exchanged NaMordenite samples. TPR results revealed that highly dispersed Ag_2O particles and Ag^+ ions located inside the structure channels are present in the catalysts. Ag_2O species can be easily reduced by adsorbed NO, as shown in the TPD experiments after adsorption of NO at room temperature.

FTIR measurements during butane adsorption show weak interactions of the hydrocarbon with silver and sodium species, and they disappear after helium sweep at 150 °C. However, when NO/He is fed, low-temperature reactions yield the formation of (–NCO) and Ag^+–(NOx)–CO species.

Toluene interactions with $Ag(x)M$ catalysts are stronger, showing the presence of the characteristic bands of aromatic ring and methyl groups interacting with Ag^+ and Na^+ ions. Adsorbed toluene molecules are held even at 400 °C. Besides, the appearance of carboxylic groups at temperatures higher than 300 °C indicates the toluene partial oxidation, probably on Ag_2O sites.

Adsorbed toluene reacts with the NO gas phase, forming organic nitrocompunds (R–NO_2), isocyanate, cyanide and isocyanide species adsorbed on Ag, that could be intermediates during the NOx-SCR reaction.

The presence of water inhibits the formation of NO_2 species and the hydrocarbon adsorption on Na^+ sites, but does not affect the toluene–Ag^+ interaction.

Acknowledgements The authors wish to acknowledge the financial support received from UNL, CONICET and ANPCyT. Thanks are given to Dr. María Alicia Ulla for helpful discussions about FTIR topics and to Elsa Grimaldi for the English language editing.

References

Baek, S.W., Kim, J.R., Ihm, S.K.: Design of dual functional adsorbent/catalyst system for the control of VOC's by using metal-loaded hydrophobic Y-zeolites. Catal. Today **93–95**, 575–581 (2004)

Berndt, H., Ritcher, M., Gerlach, T., Baerns, M.: Influence of Brønsted acidity on the redox properties of silver species in zeolite mordenite. J. Chem. Soc. Faraday Trans. **94**, 2043–2046 (1998)

Bethke, K.A., Kung, H.H.: Supported Ag catalysts for the Lean Reduction of NO with C_3H_6. J. Catal. **172**, 93–102 (1997)

Dorado, F., De Lucas, A., García, P.B., Romero, A., Valverde, J.L., Asencio, I.: SCR of NO by propene on monometallic (Co or Ni) and bimetallic (Co/Ag or Ni/Ag) mordenite-based catalysts. Ind. Eng. Chem. Res. **44**, 8988–8996 (2005)

Hadjiivanov, K.I.: IR study of CO and NOx sorption on Ag-ZSM-5. Microporous Mesoporous Mater. **24**, 41–46 (1998)

Hadjiivanov, K.I.: Identification of neutral and charged N_xO_y surface species by IR spectroscopy. Catal. Rev. Sci. Eng. **42**, 71–144 (2000)

Hadjiivanov, K.I., Vayssilov, G.N.: Characterization of oxide surface and zeolites by carbon monoxide as an IR probe molecule. Adv. Catal. **47**, 307–511 (2002)

Henriques, C., Marie, O., Thibault-Starzyk, F., Lavalley, J.C.: NO^+ ions as IR probes for the location of OH groups and Na^+ ions in main channels and side pockets of mordenite. Microporous Mesoporous Mater. **50**, 167–171 (2001)

Iliyasm, A., Zahedi-Niaki, M.H., Eic, M., Kaliaguine, S.: Control of hydrocarbon cold-start emissions: A search for potential adsorbents. Microporous Mesoporous Mater. **102**, 171–177 (2007)

Lucolano, F., Aprea, P., Caputo, D., Colella, C., Eic, M.: Adsorption and diffusion of propane and propylene in Ag^+ impregnated MCM-41. Adsorption **14**, 241–246 (2008)

Kanasawa, T.: Development of hydrocarbon adsorbents, oxygen storage materials for three-way catalysts and NOx storage-reduction catalyst. Catal. Today **96**, 171–177 (2004)

Kulkulska-Zajac, E., Datka, J.: The IR studies of the interaction of organic molecules with Ag^+ ions in zeolites. Microporous Mesoporous Mater. **109**, 49–57 (2008)

Liu, X., Lampert, J.K., Arendarskiia, D.A., Farrauto, R.J.: FT-IR spectroscopic studies of hydrocarbon trapping in Ag^+-ZSM-5 for gasoline engines under cold-start conditions. Appl. Catal. B, Environ. **35**, 125–136 (2001)

Malka-Edery, A., Abdallah, K., Grenier, P.H., Meunier, F.: Influence of traces of water on adsorption and diffusion of hydrocarbons in NaX zeolite. Adsorption **7**, 17–25 (2001)

Mortier, W.J.: Temperature-dependent cation distribution in dehydrated calcium-exchanged mordenite. J. Phys. Chem. **81**, 1334–1338 (1977)

Müslehiddinoglu, J., Vannice, M.A.: Adsorption of 1,3-butadiende on supported and promoted silver catalysts. J. Catal. **222**, 214–226 (2004)

Poucher, C.J.: The Aldrich Library of Infrared Spectra. Misconsin, USA (1981)

Oliveira, M.L.M., Miranda, A.A.L., Barbosa, C.M.B.M., Cavalcante, C.L. Jr., Azevedo, D.C.S., Rodriguez-Castellón, E.: Adsorption of thiophene and toluene on NaY zeolites exchanged with Ag(I), Ni(I) and Zn(II). Fuel **88**, 1885–1892 (2009)

Park, J.H., Park, S.J., Nam, I.S., Yeo, G.K., Kil, J.K., Youn, Y.K.: Promising zeolite-type hydrocarbon trap catalyst by a knowledge-based combinatorial approach. Microporous Mesoporous Mater. **101**, 264–270 (2007)

Parvulescu, V.I., Grange, P., Delmon, B.: Catalytic removal of NO. Catal. Today **46**, 233–316 (1998)

Sarshar, Z., Zahedi-Niaki, M.H., Huang, Q., Eic, M., Kaliaguine, S.: MTW zeolites for reducing cold-start emissions of automobile exhaust. Appl. Catal. B, Environ. **87**, 37–45 (2009)

Schoonheydt, R.A., Vandamme, L.J., Jacobs, P.A., Uytterhoeven, J.B.: Chemical, surface and catalytic properties of nonstoichiometrically exchanged zeolites. J. Catal. **43**, 292–303 (1976)

Shimizu, K., Shibata, J., Yoshida, H., Satsuma, A., Hattori, T.: Silver-alumina catalysts for selective reduction of NO by higher hydrocarbons: structure of active sites and reaction mechanism. Appl. Catal. B, Environ. **30**, 151–162 (2001)

Son, G.S., Yun, S.W., Kim, D.J., Lee, K.Y.: A study of HC reduction with hydrocarbon adsorber systems. KSME Int. J. **14**, 1168–1177 (2000)

Tamm, S., Ingelsten, H.H., Palmqvist, A.E.C.: On the different roles of isocyanate and cyanide species in propene-SCR over silver/alumina. J. Catal. **255**, 304–312 (2008)

Thibault-Starzyk, F., Seguin, E., Thomas, S., Daturi, M., Arnolds, H., King, D.A.: Real-time infrared detection of cyanide flip on silver-alumina NOx removal catalyst. Science **324**, 1048–1051 (2009)

Wesson, P.J., Snurr, R.Q.: Modified temperature programmed desorption evaluation of hydrocarbon trapping by CsMOR zeolite under cold start conditions. Microporous Mesoporous Mater. **125**, 35–38 (2009)

Wichterlová, B., Sazama, P., Breen, J.P., Burch, R., Jill, C., Capek, L., Sobalík, Z.: An in situ UV-Vis and FTIR spectroscopy study of the effect of H_2 and CO during the selective catalytic reduction of nitrogen oxides over a silver alumina catalyst. J. Catal. **235**, 195–200 (2005)

Yeom, Y.H., Li, M., Sachtler, W.M.H., Weitz, E.: Low-temperature NOx reduction with ethanol over Ag/Y: A comparison with Ag/γ-Al_2O_3 and BaNa/Y. J. Catal. **246**, 413–427 (2007)

Yeon, T.H., Han, H.S., Park, E.D., Yie, J.E.: Adsorption and desorption of hydrocarbons in multi-layered hydrocarbon traps. Microporous Mesoporous Mater. **119**, 349–355 (2009)

Zhanpeisov, N.U., Martra, G., Ju, W.S., Matsuoka, M., Coluccia, S., Anpo, M.: Interaction of N_2O with Ag^+ ion-exchanged zeolites: an FTIR spectroscopy and quantum chemical ab initio and DFT studies. J. Mol. Catal. A, Chem. **201**, 237–246 (2003)